Self-Attention Augmented Wasserstein Generative Adversarial Network-based Detection of Brain Alzheimer Disease Using MRI

SM Zakariya[1]*, Mohammad Sarosh Umar[2]

[1]Electrical Engineering Section, University Polytechnic, Aligarh Muslim University, Aligarh, India, [2]Department of Computer Engineering, ZHCET, Aligarh Muslim University, Aligarh, India . *Corresponding Author's Email: smzakariya.ubp@amu.ac.in

Abstract

Alzheimer's disease (AD) is a progressive neurological condition that leads to dementia. This study presents the Self-Attention Augmented Wasserstein Generative Adversarial Network (SAA-WGAN) for classifying AD stages, utilizing images from the Alzheimer's disease Neuroimaging Initiative (ADNI). Input images were pre-processed with Fast Guided Median Filter (FGMF) to enhance quality and reduce noise. Data augmentation techniques, including rotations and cropping, addressed class imbalances and improved training diversity. The SAA-WGAN model was validated across varying batch sizes, employing both augmented and non-augmented datasets to assess generalization capabilities. The technique was applied to 1,296 images, achieving a peak accuracy of 99% and demonstrating improved performance over conventional methods in key metrics such as AUC, Precision, and Sensitivity. These results highlight the model's effectiveness and potential to enhance diagnostic accuracy for Alzheimer's disease stages.

Keywords: ADNI Dataset, Alzheimer's Disease, Batch Size, Data Augmentation, Deep Learning, Generative Adversarial Network.

Introduction

Alzheimer's disease (AD) is a neurodegenerative disorder characterized by the progressive death of brain cells, leading to dementia and cognitive decline. Diagnosing AD is challenging and time-consuming, resulting in delayed treatment and less effective outcomes. Early diagnosis is crucial for improving treatment efficacy (1-3). As the most common type of dementia, AD predominantly affects individuals aged 65 and older (4). Advancements in diagnostic technologies can facilitate better treatment discovery and potentially reduce healthcare costs through timely interventions (5, 6). Recent developments in clinical imaging technologies, particularly MRI, have significantly enhanced the diagnosis of AD. MRI stands out due to its high spatial resolution, allowing for detailed visualization of brain structures and identifying degeneration in specific cortical regions (7-9). As the global population ages, the prevalence of AD is expected to rise dramatically over the next two decades, further burdening society (10). MRI scans often reveal structural changes that can precede overt cognitive symptoms, providing critical windows for early diagnosis (11, 12). Integrating neuroimaging and advancements in machine learning algorithms has improved the accuracy of AD diagnosis and opened new avenues for research (13, 14). Furthermore, understanding the impact of batch size and data redundancy on model performance is essential for enhancing detection methods. Techniques such as data augmentation—through rotations, flips, and contrast correction—can increase training data diversity and address the limitations of small labeled datasets in medical imaging (15). The remainder of this paper is organized into the following sections. The section titled 'Related Work' reviews existing approaches to classification in Alzheimer's disease (AD). 'Methodology' outlines the suggested method, detailing the processing of AD and the classification techniques used. 'Results and Discussion' presents the model's performance results along with an in-depth analysis. Finally, the 'Conclusion' summarizes the key findings of the study. A transfer learning-based CNN with data augmentation was applied to 3D MRI scans from the OASIS dataset to solve the class imbalance problem. It uses pre-trained models for

feature extraction, improving accuracy without requiring a large, evenly distributed dataset. The main advantage is its ability to achieve high classification accuracy (16). However, relying on data augmentation to compensate for class imbalance was a limitation that may not fully generalize to other datasets or real-world scenarios. A CNN model-based classification framework produced decreased overfitting, memory utilization, computational complexity, and better accurate classifications for AD stages. The VGG16 model, fine-tuned from ImageNet, achieved the best accuracy. The main advantage was high accuracy with minimal labeled data and computational resources (17). However, a limitation was that the transfer learning method does not generalize well to unobserved data without extensive refinement.

Brain MRI images are classified for AD using the ADNet-DA model (with domain adaption). The approach uses CNNs to automatically identify AD biomarkers without needing prior domain-specific knowledge. ADNet-DA outperformed numerous prior techniques with its exceptional accuracy in the CAD Dementia challenge testing. A major advantage was its fully automatic, fast process for detecting AD-related changes in brain images (18). However, accuracy leaves room for improvement, especially by adapting the model to different datasets to improve its diagnostic accuracy. A thorough examination of medical image augmentation approaches provides comparisons and interpretations, exploring the strategies employed to improve further deep learning models' abilities to diagnose diseases in an array of organs, including the eyes, brain, lungs, and breasts. Several types of imaging, such as fundoscopy, MRI, CT, and mammography, are employed with these techniques (19). However, the study lacks clarity regarding which augmentation techniques are most effective for specific image types, as the results vary widely due to differences in diseases, network architectures, and the number of datasets used.

Three data augmentation techniques using various CNN models and transformation layers were evaluated and reported for the 3D CNN models. The studies used multiple testing and cross-validation to overcome the data paucity and variability. Models with an intermediate level of complexity produced consistent results at different

folds and trial counts, making them the top-performing models (20). However, accuracy was decreased when utilizing concurrent increments, and up to 10% of the difference in model performance might be attributed to strategy and design. The AD phases were classified using ADD-Net, a framework with fewer parameters that is optimized for training on small datasets. Synthetic hypersampling was used to guarantee a balanced class distribution in order to overcome class imbalance in the Kaggle MRI dataset. ADD-Net demonstrated superior performance across several metrics, surpassing models like DenseNet169, VGG19, and InceptionResNet V2 (21). However, the model's reliability in synthetic data augmentation may not fully generalize to real-world, highly heterogeneous datasets. An efficient CNN model based on InceptionV3 was developed to classify the stages of Alzheimer's disease (AD) using the ADNI dataset. Data augmentation was employed together with the CLAHE approach for image improvement to rectify the imbalance in classes. AlzheimerNet achieved the highest accuracy and outperformed five pre-trained models (22). However, the reliance on data augmentation and fine-tuning limits generalizability to other datasets with distinct characteristics. This study tackles these challenges by introducing the Self-Attention Augmented Wasserstein Generative Adversarial Network (SAA-WGAN). The model improves image quality through advanced pre-processing with the Fast Guided Median Filter (FGMF), uses data augmentation to balance classes and enhance training diversity, and features an innovative architecture that delivers exceptional accuracy.

Methodology

In this study, SAA-WGAN is projected to classify AD stages at different batch sizes with and without augmentation. The input images are initially attained from the ADNI database (23). The images are preprocessed using Fast Guided Median Filter (FGMF) to improve image quality by effectively reducing noise and enhancing image features for more accurate classification (24). Besides, to address the imbalanced data and increase the diversity of training data, data augmentation techniques, including rotations, and crop adjustments, are employed. Also, a SAA-WGAN framework is presented for the classification of AD stages (25). The model is validated at different

batch sizes to assess its stability, performance, and computational efficiency. Additionally, the dataset's augmented and non-augmented versions are used to validate the data augmentation effect on the method generalization capabilities. The process of the presented methodology is represented in Figure 1.
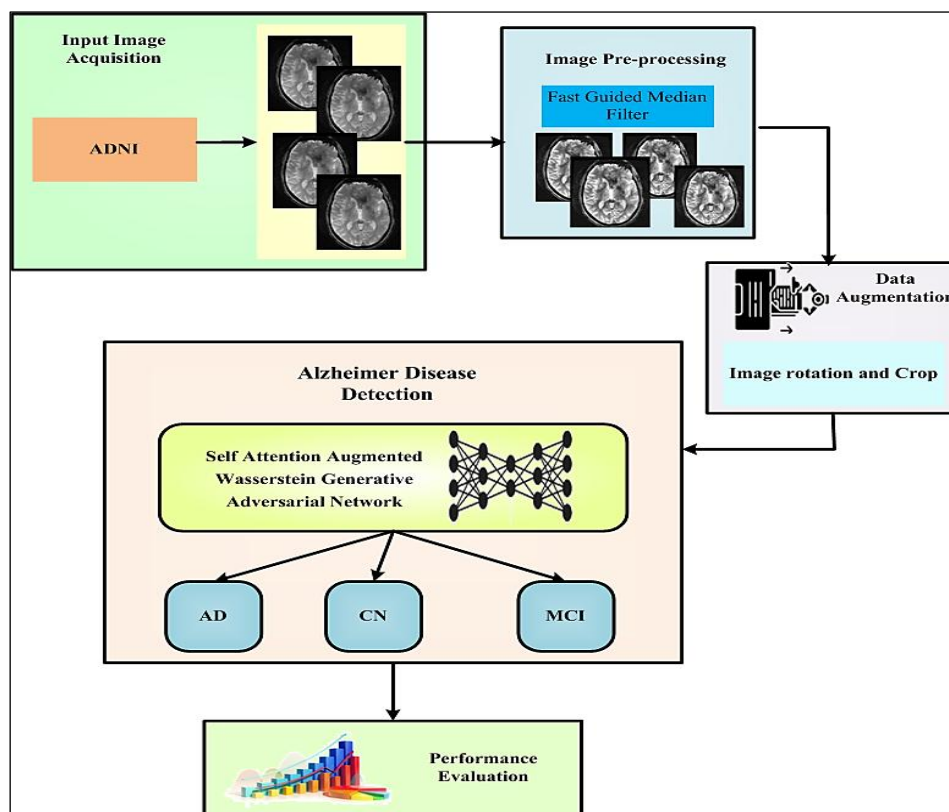
Figure 1: Block Diagram Representation of the Projected Model

Data acquisition involves different categories of images like molecular brain images, structural brain images, functional brain images, genetic data, demographic information, and cognitive assessments. The ADNI dataset primarily consists of participants aged 55 and older, with a roughly equal distribution between men and women. Cognitive status among participants ranges from cognitively normal (CN) to Alzheimer's disease (AD), covering various stages of mild cognitive impairment (MCI). Table 1 describes the ADNI demographic information.

Table 1: ADNI Dataset Demographic Information

Parameters	CN	MCI	AD
Images	2665	3924	1731
Subjects	110	125	129
Males	1400 (52.6%)	2080 (53.1%)	900 (51.9%)
Females	1265 (47.4%)	1844 (46.9%)	831 (48.1%)
Age (years)	51-90	55-89	60-89
Mean (Age)	72.5	74.2	76.8

In this stage, the input brain images are preprocessed using Fast Guided Median Filter (FGMF) to remove the image noise. The FGMF enhances the traditional guided filter, designed to reduce noise while preserving important image details efficiently. It uses local statistics to adaptively filter the image. Initially, the guided filter formulation for the guided image (I) the output filtered image (O) can be computed as using equation [1],

$$O(x) = a(x) * I(x) + b(x)$$
[1]

Where, $O(x)$ indicates the output pixel value, $I(x)$ specifies the input pixel value, $a(x)$ and $b(x)$ represents the filter parameters that need to be computed. These parameters are determined based on the local image statistics. To calculate $a(x)$ and $b(x)$ there is a need to compute the local mean ($Mean_I$) and local covariance (Cov_I) of the guided image [I] within a local window of size ($w \times w$) centered at pixel x. The mean and covariance are calculated as follows using equations [2] and [3],

$$Mean_{I(x)} = \left(\frac{1}{w^2}\right) * \sum I(P)$$
[2]

$$Cov_{I(x)} = \left(\frac{1}{w^2}\right) * \sum I(P) * I(P)^T$$
[3]

Where, P indicates the pixels within the local window. Once the local mean and covariance are computed then the filter parameters $a(x)$ and $b(x)$ are calculated using equations [4] and [5] as follows,

$$a(x) = \frac{\left(Cov_{I(x)} + \varepsilon * I(x)\right)}{\left(Var_{I(x)} + \varepsilon\right)}$$
[4]

$$b(x) = Mean_{I(x)} - a(x) * Mean_{I(x)}$$
[5]

Where, ε represents a small positive constant to prevent division by zero, and $Var_{I(x)}$ represents the local variance of the guided image [I] within the window and is computed using equation [6],

$$Var_{I(x)} = Cov_{I(x)} - Mean_{I(x)} * Mean_{I(x)}^T$$
[6]

Finally, by using the computed $a(x)$ and $b(x)$ to filter the noisy input image (P) to obtain the denoised output image (Q) as represented in equation [7] as follows,

$$Q(x) = a(x) * P(x) + b(x)$$
[7]

At last, the developed FGMF effectively reduce the noise while preserving important image features. The input and preprocessed images are shown in Figure 2.
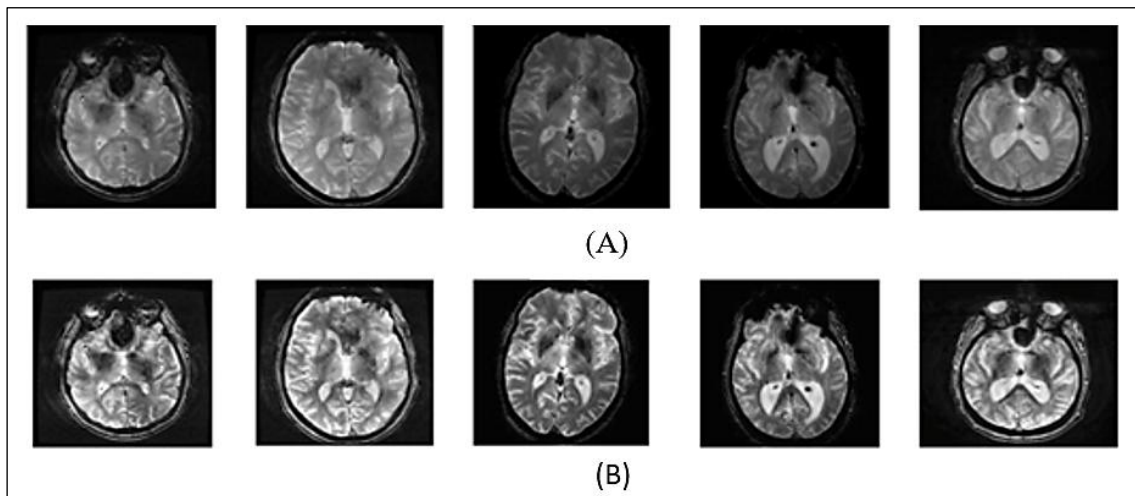
Figure 2: (A) Input Brain Images (B) Preprocessed Images

A large and diverse dataset is essential to train effective models in deep learning. Image augmentation is a technique for artificially expanding the dataset's size and diversity through various transformations applied to the original images. This technique increases generalization, reduces the risk of overfitting, and sometimes even enhances general performance and reliability. In this study, some augmentation techniques were applied to the preprocessed images, as mentioned in Table 2.

Table 2: Data Augmentation Hyperparameters

Augmentation Technique	Parameters
Image Rotation	90^0, 180^0, 270^0
Crop From Top	90^0, 180^0, 270^0

Crop From Bottom	90^0, 180^0, 270^0
Crop From Right	90^0, 180^0, 270^0
Crop From Left	90^0, 180^0, 270^0
Whole Crop	90^0, 180^0, 270^0
Crop From Corner	90^0, 180^0, 270^0

Such variations result in the duplication of images for all the originals. This leads to a relatively large dataset and, as a result, a more significant training set. This more extensive as well as diversified set helps the deep learning model to learn more associated patterns with the data, which tends to gain an increased accuracy in classifying stages of Alzheimer's disease. After such an augmentation process, the dataset became much larger by containing a significantly larger number of images. The augmented images are therefore depicted in Figure 3.
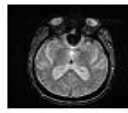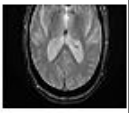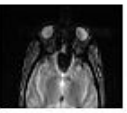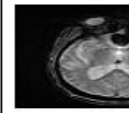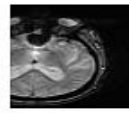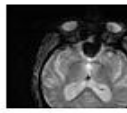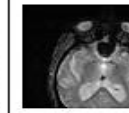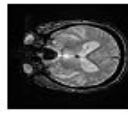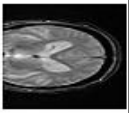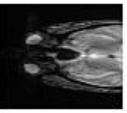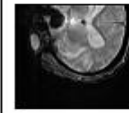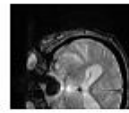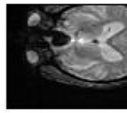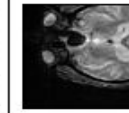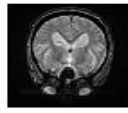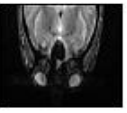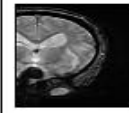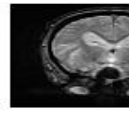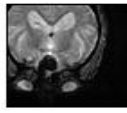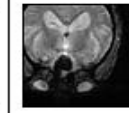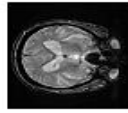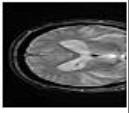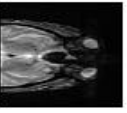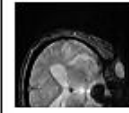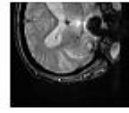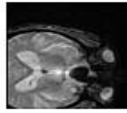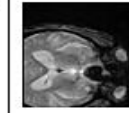
Figure 3: Augmented Output Images

SAA-WGAN Model for Alzheimer's Detection

A SAA-WGAN is regarded as the state-of-the-art model, for which key aspects, including self-attention and Wasserstein GANs are said to augment medical image analysis, particularly partially the Alzheimer's diagnosis. The WGAN meticulously polishes the conventional technique of GAN, and its main principle is the improvement of the discriminator by increasing the distances between the real and the generated data as measured by Wasserstein distance. This especially helps in regulating the learning process of GANs and also enhances the variation in the data created. In a traditional GAN, the objective is to find the generator (g) that produces realistic data such that the discriminator (d) cannot distinguish between the real and generated data. The GAN's min-max optimization problem is given in equation [8],

$$\min_{g}\max_{d} - \left(-E(d(k,y)) + E(d(k,Y)) \right)$$

[8]

Where, the input brain images are denoted as y, the augmented images are denoted as Y, and the groundtruth images are mentioned as k. In this, the

loss of discriminator is calculated using equation [9],

$$loss_d = -E(d(k,y)) + E(D(k,Y))$$

[9]

Also, the loss of modified generator is computed using equation [10],

$$loss_g = -E(d(k,Y))$$

[10]

Self-attention allows the model to attend to important parts of the input by computing attention scores that capture long-range dependencies between different parts of the image. Such images, for example, MRI or PET scans of medical images, bring about a significant challenge because the subtle patterns in various regions of the brain can indicate whether a person has Alzheimer's disease. In the self-attention mechanism, there is a weighted sum of values whose weights are computed dynamically based on the similarity between queries and keys. The formula of self-attention is given in equation [11],

$$Att(q,k,v) = soft\left(\frac{qk^T}{\sqrt{D_k}}\right)v$$

[11]

Where, q denotes the queries that is represented as $q = yw_q$ with input data y and weight matrix W_q, k denotes the keys that is represented as $k = yw_k$, v denotes the values that is represented as $q = yw_v$, and the key dimensionality is denoted as D_k. The self-attention mechanism is integrated with convolutional layers in Attention-Augmented Convolution. This is useful in processing medical images, where the model needs to simultaneously capture local features (via convolution) and global dependencies (via self-attention).

The output of the attention-augmented convolution is denoted in equation [12],

$$Output_{Conv}(y) = Conv(y) + Att(y)$$

[12]

Where, the output from the regular convolution is denoted as $Conv(y)$, and the self attention output is denoted as $Att(y)$. The discriminator is trained just to perform the appropriate assignment between real brain images and those generated by the generator during training. The generator is trained such that during training, its output is not distinguishable from real brain images and focuses on Alzheimer-specific features like brain atrophy because of the self-attention mechanism. The interaction of a stable training process from WGAN and the global dependencies capturing the ability of self-attention makes SAA-WGAN very effective in creating high-quality medical images and detecting Alzheimer's with high accuracy. The Wasserstein GAN framework, used for integration into SAA-WGAN to create stable training for high-quality image generation, is further enhanced with a self-attention mechanism to catch all important global dependencies for medical images. Therefore, the model essentially focuses equally on local features as well as long-range dependencies, making this particularly suitable for Alzheimer's detection. The loss functions are those that yield a high-quality, perceptually accurate image generation.

Results and Discussion

A simulation of the suggested SAA-WGAN method for AD stages classification is presented in this section. The suggested method was implemented on the Python platform, and the following performance metrics were assessed: accuracy for with augmentation and without augmentation, likewise precision rate, sensitivity rate, specificity value, ROC, and F-measure. Here, the suggested SAA-WGAN methodology is compared with existing methods such as, AlexNet-CNN (21), VGG16-CNN (22), and ADNet-DA (23) respectively.

Metrics for Performance Evaluation

Here, the efficiency of the SAA-WGAN methodology is analysed by various performance metrics such as accuracy with augmentation and without augmentation, likewise precision rate, sensitivity rate, specificity value, ROC, and F-measure. It needs parameters like True Negative $(T(N))$, True Positive $(T(P))$, False Negative $(F(N))$, and False Positive $(F(P))$.

Accuracy measures the effectiveness of a classification model in accurately categorizing AD into correct categories, which can be computed using equation [13].

$$Acc = \frac{T(N)+T(P)}{F(P)+F(N)+T(P)+T(N)}$$

[13]

Precision estimates the extent of accurately anticipated positive examples out of all emphatically predicted samples, which is registered utilizing an equation [14],

$$Pr \ Pr = \frac{T(P)}{T(P)+T(N)}$$

[14]

Recall measures the quantity of appropriately prophesied positive models out of entirely true

positive models in the given dataset that is computed based on equation [15].

$$= \frac{T(P)}{T(P)+F(N)}$$

[15]

F-measure is often used when there is an imbalance among the positive as well as negative

samples or when there is a need to prioritize both precision and recall equally, which is calculated using equation [16].

$$F - measure = \frac{2(\times PrPr)}{+ Pr}$$

[16]
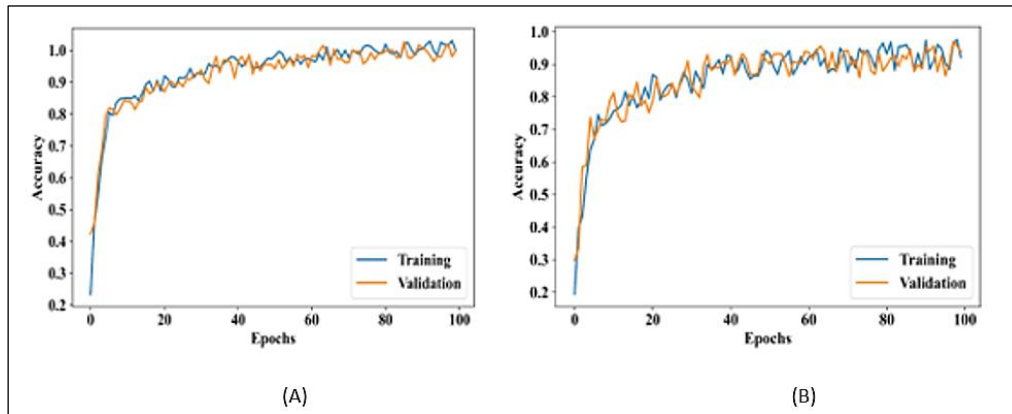
Figure 4: Accuracy for Suggested Model (A) with Augmentation and (B) Without Augmentation Using the ADNI dataset
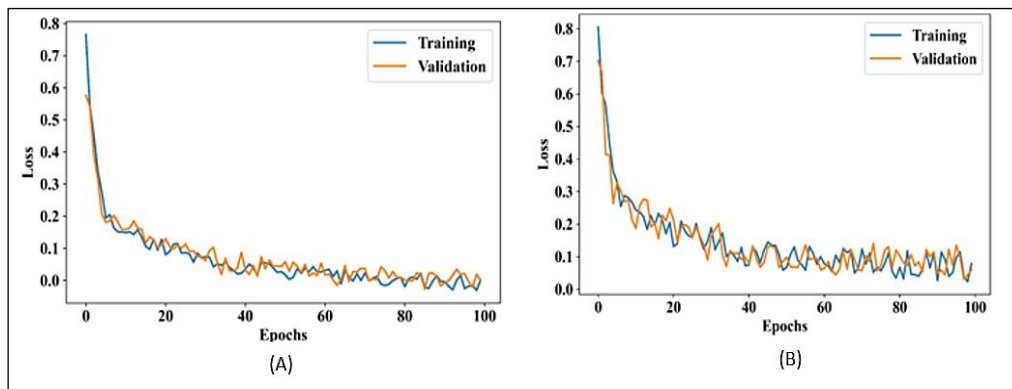
Figure 5: Loss for Suggested Model (A) with Augmentation and (B) Without Augmentation Using the ADNI dataset

Figure 4 and Figure 5 shows the connection between accuracy and loss for the Suggested Model before and after applying augmentation techniques using the ADNI dataset. As training progresses, the accuracy improves while the loss decreases, indicating effective learning and model convergence. This trend demonstrates the model's ability to accurately detect AD while reducing errors.

Comparative Analysis

In this study, the comparative analysis of the SAA-WGAN methodology is explained. The performance metrics of the suggested SAA-WGAN methodology is compared with existing methods such as, AlexNet-CNN (21), VGG16-CNN (22), and ADNet-DA (23) respectively.
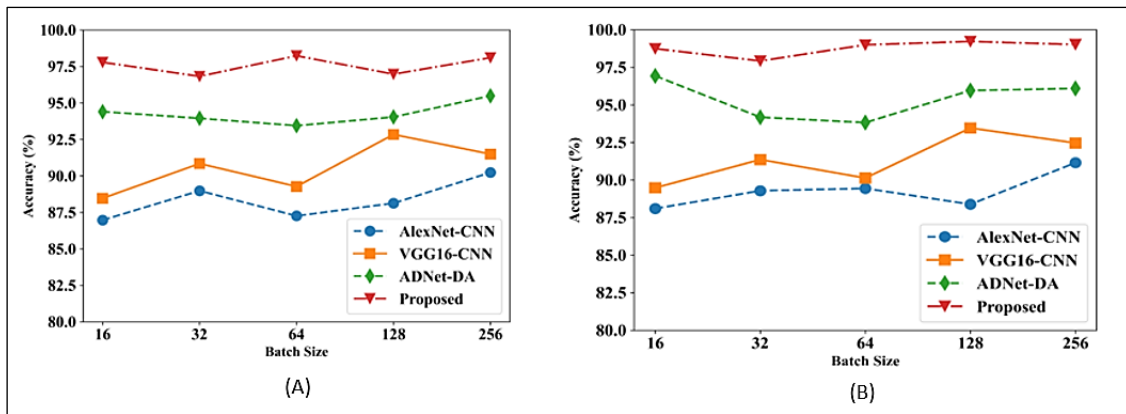
Figure 6: Performance Analysis of Accuracy (A) Without Augmentation and (B) With Augmentation

The accuracy comparison for without and with augmentation model is shown in Figure 6. Here, the SAA-WGAN methodology achieves higher accuracy rate as 99 % using augmentation approach and outperforms than other conventional techniques like AlexNet-CNN, VGG16-CNN, and ADNet-DA respectively.

Table 3: Comparative Analysis of Performance Metrics

Parameters		AlexNet-CNN	VGG16-CNN	ADNet-DA	Proposed Method
Without augmentation	Accuracy	90.23	91.49	95.29	98.11
	Precision	91.12	92.28	95.9	98.29
	Sensitivity	91.58	92.68	96.14	98.3
	Specificity	90.76	90.9	94.82	97.13
	F-measure	91.35	92.48	96.03	98.34
With augmentation	Accuracy	91.15	92.46	96.097	99.017
	Precision	91.96	93.16	96.4	99.11
	Sensitivity	92.3	93.5	96.66	99.16
	Specificity	91.56	91.8	95.34	97.90
	F-measure	92.17	93.34	96.56	99.13

In Table 3, the performance comparison of different models for Alzheimer's detection is shown. The developed model consistently outperforms AlexNet-CNN, VGG16-CNN, and ADNet-DA in all metrics, both with and without data augmentation. The SAA-WGAN methodology achieves the highest accuracy as 99.017% and F-measure as 99.13% with augmentation, indicating superior classification performance and robustness. Augmentation further enhances the overall performance across all models.
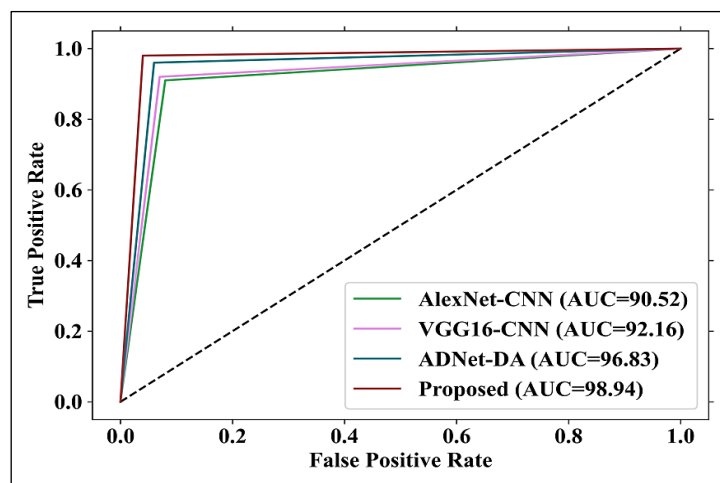
Figure 7: Performance Analysis of ROC

Figure 7 shows the ROC curve comparison. Then, the ROC of the suggested method provides 4.56%, 3.45%, and 2.63% greater AUC than other conventional approaches like AlexNet-CNN, VGG16-CNN, and ADNet-DA methods respectively.

Integration into Clinical Practice

- Clinical Collaboration: Partnering with healthcare professionals and institutions will facilitate the integration of our model into existing diagnostic workflows.
- User-Friendly Interface: Developing an intuitive software interface will streamline the submission of imaging data and provide accessible classification results.
- Training and Education: Ongoing training for clinicians will ensure their comfort with using the model and interpreting its outputs.
- Regulatory Approval: Obtaining necessary regulatory certifications will ensure compliance with medical standards and patient safety.
- Integration with EHR Systems: Our model should be compatible with existing Electronic Health Record systems to facilitate data sharing.

Challenges

- Data Quality and Availability: High-quality imaging data is essential, and variability across clinical settings may affect accuracy.
- Interpretability of Results: Clinicians require interpretable outputs to trust the model's predictions.
- Resource Constraints: Advanced models may require significant computational resources, which may not be available in smaller institutions.
- Patient Privacy: Adhering to data privacy regulations like HIPAA is crucial when deploying AI in healthcare.
- Establishing Clinical Validation: Continuous validation across diverse clinical populations is necessary to confirm the model's reliability.

By addressing these strategies and challenges, we aim to enhance diagnostic capabilities for Alzheimer's disease in clinical settings. Key improvements made in the manuscript include emphasizing the effectiveness of the SAA-WGAN model, which achieved a peak accuracy of 99% and outperformed conventional methods in metrics like AUC, Precision, and Sensitivity. Additionally, the use of pre-processing techniques (FGMF) and data augmentation were discussed in detail, showcasing their role in enhancing image quality and addressing class imbalances, as demonstrated in the results.

Conclusion

The Self-Attention Augmented Wasserstein Generative Adversarial Network (SAA-WGAN) has been successfully implemented to classify Alzheimer's disease (AD) stages using images from the ADNI database. Pre-processing with Fast Guided Median Filter (FGMF) enhanced image quality, while data augmentation techniques were employed to address class imbalances and increase training diversity. The model was validated with both augmented and non-augmented datasets at various batch sizes to assess its generalization capabilities. Comprehensive evaluations demonstrated that the SAA-WGAN method achieved an area under the curve (AUC) that exceeded traditional approaches, with improvements of 4.56%, 3.45%, and 2.63% compared to AlexNet-CNN, VGG16-CNN, and ADNet-DA, respectively. These findings highlight the effectiveness of the suggested model in enhancing classification accuracy and contribute to the advancement of diagnostic tools for Alzheimer's disease.

Abbreviations

MRI: Magnetic Resonance Imaging, CT: Computed Tomography, PET: Positron Emission Tomography, AD: Alzheimer's disease, CNN: Convolution Neural Network, AUC: Area under Curve, ROC: Receiver Operating Characteristics, SAA-WGAN: Self-Attention Augmented Wasserstein Generative Adversarial Network, ADNI: Alzheimer's disease Neuroimaging Initiative, FGMF: Fast Guided Median Filter, CLAHE: Contrast-Limited Adaptive Histogram Equalization, CAD: Supervised Computer-Aided Diagnosis.

Acknowledgment

assistance of their colleagues in accessing literature from various databases and sources.

Author Contributions

SM Zakariya: Prepared the manuscript, collected data, implemented the algorithms, analyzed the data, and reviewed the final manuscript, Mohammad Sarosh Umar: Contributed to the conception and interpretation of results, provided corrections, and edited and reviewed the final manuscript.

Conflict of Interest

The authors declare no competing financial interests or personal affiliations that could have influenced this study.

Ethics Approval

The dataset used in this study were publicly available and did not involve interaction with any subject. Therefore, no ethics approval was required.

Funding

This study did not receive any specific funding from public, private, or nonprofit organization.

References

1. Alof A, Khan MU. Multi-label Classification of Alzheimer's Disease Stages from Resting-state FMRI-based Correlation Connectivity Data and Deep Learning. Computers in Biology and Medicine. 2022; 151: 106240.
2. Savas S. Detecting the Stages of Alzheimer's Disease with Pre-trained Deep Learning Architectures. Arabian Journal for Science and Engineering. 2021; 47(2):2201–2218.
3. Orouskhani M, Zhu C, Rostamian S, Zadeh FS, Shafiei M, Orouskhani. Alzheimer's disease detection from structural MRI using conditional deep triplet network. Neuroscience Informatics. 2022; 2(4): 100066.
4. Dwivedi S, Goel T, Tanveer M, Murugan R, Sharma R. Multimodal Fusion-based Deep Learning Network for effective diagnosis of alzheimer's disease. IEEE MultiMedia. 2022; 29(2): 45–55.
5. Wu H, Luo J, Lu X, Zeng Y. 3D Transfer Learning Network for classification of alzheimer's disease with MRI. International Journal of Machine and Cybernetics. 2022; 13(7): 1997–2011.
6. Lu B, Li HX, Chang ZK, Li L, Chen NX, Zhu ZC, Zhou HX, Li XY, Wang YW, Cui SX, Deng ZY. A practical Alzheimer's disease classifier via brain imaging-based deep learning on 85,721 samples. Journal of Big Data. 2022 Oct 13;9(1):101. https://doi.org/10.1186/s40537-022-00650-y
7. Zhang F, Pan B, Shao P, Liu P, Shen S, Yao P, Xu RX. A Single Model Deep Learning Approach for Alzheimer's Disease Diagnosis. Neuroscience. 2022; 491:200-214.
8. Sharma R, Goel T, Tanveer M, Murugan R. FDN-ADNet: Fuzzy LS-TWSVM based deep learning network for prognosis of the alzheimer's disease using the sagittal plane of MRI scans. Applied Soft Computing. 2022; 115: 108099.
9. Hu Y, Wen C, Cao G, Wang J, Feng Y. Brain Network connectivity feature extraction using Deep Learning for Alzheimer's Disease Classification. Neuroscience Letters. 2022; 782: 136673.
10. Odusami M, Maskeliūnas R, Damaševičius R, Misra S. Explainable deep-learning-based diagnosis of alzheimer's disease using multimodal input fusion of PET and MRI images. Journal of Medical and Biological Engineering. 2023; 43(3): 291–302.
11. Suresha HS and Parthasarathy SS. Detection of Alzheimer's disease using grey wolf optimization-based clustering algorithm and deep neural network from magnetic resonance images. Distributed and Parallel Databases. 2022; 40(4): 627-655.
12. SinhaRoy R and Sen A. A Hybrid Deep Learning Framework to Predict Alzheimer's Disease Progression using generative adversarial networks and deep convolutional neural networks. Arabian Journal for Science and Engineering. 2024 Mar;49(3):3267-84.
13. Habuza T, Zaki N, Mohamed EA, Statsenko Y. Deviation from model of normal aging in alzheimer's disease: Application of deep learning to structural MRI data and cognitive tests. IEEE Access. 2022; 10: 53234–53249.
14. Papadimitriou O, Kanavos A, Mylonas P, Maragoudakis M. Classification of alzheimer's disease subjects from MRI using deep convolutional neural networks. Lecture Notes in Networks and Systems. 2023; 277–286. http://dx.doi.org/10.1007/978-3-031-44146-2_28
15. Kumari R, Das S, Singh RK. Agglomeration of deep learning networks for classifying binary and multiclass classifications using 3D MRI images for early diagnosis of alzheimer's disease: A feature-node approach. International Journal of System Assurance Engineering and Management. 2023; 15(2): 931–949.
16. Afzal S, Maqsood M, Nazir F, Khan U, Aadil F, Awan KM, Mehmood I, Song OY. A data augmentation-based framework to handle class imbalance problem for Alzheimer's stage detection. IEEE access. 2019; 7: 115528-115539.
17. Arafa DA, Moustafa HED, Ali HA, Ali-Eldin AM, Saraya SF. A deep learning framework for early diagnosis of Alzheimer's disease on MRI images. Multimedia Tools and Applications. 2024; 83(2): 3767-3799.
18. Folego G, Weiler M, Casseb RF, Pires R, Rocha A. Alzheimer's disease detection through whole-brain 3D-CNN MRI. Frontiers in bioengineering and biotechnology. 2020 Oct 30;8:534592.
19. Goceri E. Medical image data augmentation: techniques, comparisons and interpretations. Artificial Intelligence Review. 2023 Nov;56(11):12561-605.
20. Turrisi R, Verri A, Barla A. The effect of data augmentation and 3D-CNN depth on Alzheimer's Disease detection. arXiv preprint

arXiv:2309.07192. 2023 Sep 13. https://arxiv.org/abs/2309.07192

21. Fareed MM, Zikria S, Ahmed G, Mahmood S, Aslam M, Jillani SF, Moustafa A, Asad M. ADD-Net: an effective deep learning model for early detection of Alzheimer disease in MRI scans. IEEE Access. 2022 Sep 5;10:96930-51.

22. Shamrat FJ, Akter S, Azam S, Karim A, Ghosh P, Tasnim Z, Hasib KM, De Boer F, Ahmed K. AlzheimerNet: An effective deep learning based proposition for alzheimer's disease stages classification from functional brain changes in magnetic resonance images. IEEE Access. 2023 Feb 14;11:16376-95.

23. Vallabh N. ADNI MRI Images. Kaggle website. 2024. https://www.kaggle.com/datasets/vallabhaneniu day/adni-mri-images

24. Mishiba K. Fast guided median filter. IEEE Transactions on Image Processing. 2023 Jan 5;32:737-49.

25. Shang Z, Zhang J, Li W, Qian S, Liu J, Gao M. A novel small samples fault diagnosis method based on the self-attention Wasserstein generative adversarial network. Neural Processing Letters. 2023 Oct;55(5):6377-407.